JACS
JOURNAL OF THE AMERICAN CHEMICAL SOCIETY

Communication

pubs.acs.org/JACS

Fast and Persistent Electrocatalytic Water Oxidation by Co–Fe Prussian Blue Coordination Polymers

Sara Pintado,[†,§] Sara Goberna-Ferrón,[†,§] Eduardo C. Escudero-Adán,[†] and José Ramón Galán-Mascarós*[,†,‡]

[†]Institute of Chemical Research of Catalonia (ICIQ), Av. Paisos Catalans 16, E-43007 Tarragona, Spain

[‡]Catalan Institution for Research and Advanced Studies (ICREA), Passeig Lluis Companys, 23, E-08010, Barcelona, Spain

Supporting Information

ABSTRACT: The lack of an efficient, robust, and inexpensive water oxidation catalyst (WOC) is arguably the biggest challenge for the technological development of artificial photosynthesis devices. Here we report the catalytic activity found in a cobalt hexacyanoferrate (CoHCF) Prussian blue-type coordination polymer. This material is competitive with state-of-the-art metal oxides and exhibits an unparalleled long-term stability at neutral pH and ambient conditions, maintaining constant catalytic rates for weeks. In addition to its remarkable catalytic activity, CoHCF adds the typical properties of molecule-based materials: transparency to visible light, porosity, flexibility, processability, and low density. Such features make CoHCF a promising WOC candidate for advancement in solar fuels production.

Water splitting is a general chemical problem and a crucial step in the development of artificial photosynthesis. Two catalysts are needed, one for the oxidation of water into O_2, and another one for the reduction of protons to H_2. Water oxidation catalysis remains the biggest challenge because of its high kinetic barrier and high oxidation potential (eq 1), and the

$$2H_2O \rightarrow O_2 + 4H^+ + 4e^-,$$
$$E = +1.229 - 0.059(\mathrm{pH})\ \mathrm{V\ vs\ NHE\ at\ 25^\circ C} \quad (1)$$

number of electrons involved. A cost-efficient catalyst able to work at low overpotential for optimized energy conversion will also need to be stable to air, light, water, heat, and oxidative deactivation. Many research groups are currently working on homogeneous and heterogeneous water oxidation catalysts (WOCs), looking for fast, stable, and inexpensive candidates.[1−3]

Heterogeneous catalysts have the advantage of higher stability and easier implementation into devices. In this field, only transition metal oxides appear as viable candidates,[4−9] with the state-of-the-art defined by highly active cobalt oxide films.[10−22] In the search for WOC activity in other solid-state structural types, we turned our attention to cyanide-bridged coordination polymers.

Transition metal hexacyanometallates (MHCMs)[23] are isostructural to the original Prussian blue, the all-iron $Fe^{III}_4[Fe^{II}(CN)_6]_3{\cdot}xH_2O$ derivative discovered over 300 years ago as a pigment. In the crystal structure, two octahedral metal centers are bound through cyanide bridges to construct a face-centered cubic unit cell (Figure 1).[24] MHCMs are known for many combinations of transition metal ions in multiple oxidation states. They are also highly porous and incorporate interstitial solvent molecules and alkali metal ions. Despite their rigid structure, these coordination polymers are usually non-stoichiometric because different non-integer ratios can be accommodated. This chemical variety makes them a versatile type of molecule-based materials. Indeed, after decades of MHCM chemistry, they are still the subject of frontier research in very different fields.[25−29] Here we report the water oxidation catalytic activity found in Prussian blue-type cobalt hexacyanoferrate (CoHCF)-modified electrodes.

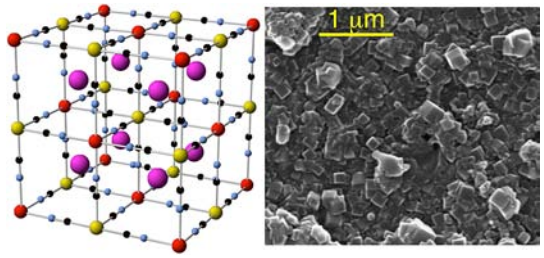

Figure 1. (Left) Representation of a cubic Prussian blue-type structure (transition metal, yellow/red; C, black; N, blue; interstitial open sites, purple). (Right) SEM image of a CoHCF-modified FTO electrode.

CoHCF was prepared on fluoride-doped tin oxide (FTO)-coated glass electrodes following a well-established electrochemical method (Supporting Information (SI)).[30−33] First we plated the FTO electrode with metallic cobalt by applying a reduction potential to a $CoCl_2$/water solution. The Prussian blue film was then obtained by applying a positive potential (0.5 V vs NHE) to these electrodes in a solution containing hexacyanoferrate(III). During derivatization, CoHCF crystallites deposit on the electrode. No residues of metallic cobalt remain at this stage, as confirmed by the absence of any sign of the corresponding oxidation wave (Figure S1).

The surface of the CoHCF-coated electrodes is highly transparent (Figure S2). Following this procedure, the stoichiometry of the films is reproducible: $K_{2x}Co_{(2-x)}[Fe$-

Received: June 20, 2013
Published: August 27, 2013

   dx.doi.org/10.1021/ja406242y | J. Am. Chem. Soc. 2013, 135, 13270−13273

$(CN)_6]$ ($0.85 < x < 0.95$), as confirmed by energy-dispersive X-ray (EDX) analysis (Figure S4 and Table S1). The UV−vis spectra, with the light beam passing through the glass substrate, show a minimum transmittance of 70% in the 400−900 nm region without significant absorption bands (Figure S3a). The IR spectra show one single band in the cyanide stretch region at 2076 cm^{-1} (Figure S3b), characteristic of $Fe^{II}-CN-Co^{II}$ bridges.[34] These are the two stable redox states at the derivatization potential. The morphology of the electrode surface consists of an agglomerate of cubic-shaped crystallites with maximum edges up to 0.25 μm (Figure 1). X-ray powder diffraction of these crystallites shows the typical pattern of a Prussian blue structure (Figure 2).[35] The diffraction peaks are

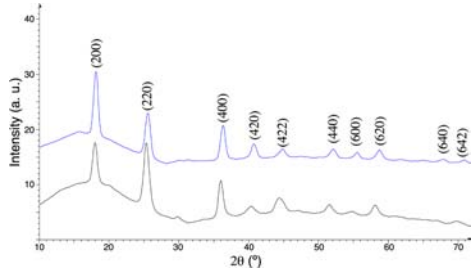

Figure 2. X-ray diffraction patterns for crystallites from a CoHCF-modified FTO electrode before (black line) and after a 5 h bulk water electrolysis (blue line).

broad due to the small particle size, and their indexation leads to a face-centered cubic unit cell parameter $a = 10.08 \pm 0.05$ Å. All experiments reported here were performed with at least three CoHCF-modified electrodes, and consistent results were found.

Cyclic voltammetry of these CoHCF-modified electrodes in 50 mM potassium phosphate (KP_i) electrolyte at neutral pH (Figure 3a) shows a quasi-reversible redox couple with the

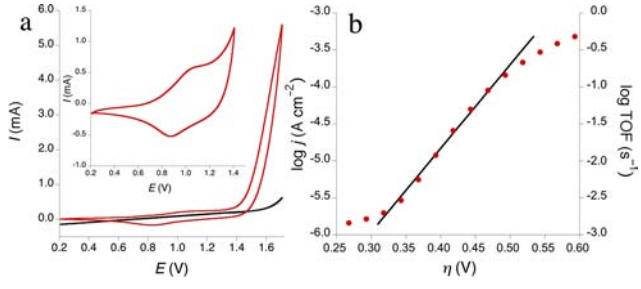

Figure 3. (a) Cyclic voltammagram of a CoHCF-modified FTO electrode in 50 mM KPi electrolyte at pH 7.0 (red line) with a 50 mV/s sweep rate. Profile for a pristine FTO electrode (black line). Inset: Detail of the 0.2−1.4 V range with a 100 mV/s sweep rate. (b) Tafel plot of the steady current density and estimated TOF at neutral pH. Calculated slope = 88 mV/decade.

oxidation peak at 1.04 V and the reduction peak at 0.87 V vs NHE ($E_{1/2} = 0.96$ V, $E_c - E_a = 170$ mV). This one-electron process can be assigned to the $Co^{II}Fe^{II}-Co^{III}Fe^{II}$ couple.[36] At higher oxidation potentials, a characteristic catalytic water oxidation wave appears.

Steady current density (j) was measured at different applied potentials in a two-compartment cell with a glass frit separation in a well-stirred neutral KP_i (50 mM) water solution containing KNO_3 (1 M) as electrolyte. Significant current was detected above 1.10 V (NHE). The Tafel plot (Figure 3b) that relates catalytic current and overpotential (η) shows linear behavior for intermediate potentials, with slopes in the 85−95 mV/decade range, confirming the catalytic process. The lower limit catalytic rates for these CoHCF-modified electrodes can be estimated by calculating the total number of redox-active sites from the cyclic voltammetry data (SI). The coverage of redox-active Co centers on the electrode is $\Gamma_0 = 1.4 \pm 0.2$ nmol/cm^2, as extracted from the linear relationship between the peak current of the Co^{III}/Co^{II} reduction wave and scan rate (Figure S5). This is an upper limit to the real number of catalytic sites, since heterogeneous catalysis should occur only on the surface of the crystallites, whereas the bulk material is electroactive. With these coverage numbers applied to the linear Tafel region, the turnover frequency (TOF) shows values between 2×10^{-3} s^{-1} at $\eta = 300$ mV and 0.5 s^{-1} at 550 mV.

We carried out bulk water electrolysis in the same experimental conditions (Figure 4). After a short induction

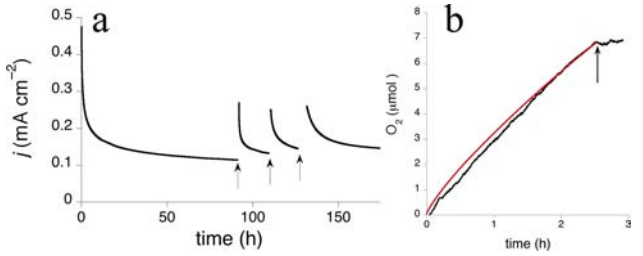

Figure 4. (a) Current profile during water electrolysis at 1.41 V (vs NHE) at pH 7.0 of a CoHCF-modified electrode. (b) Catalytic oxygen evolution (black) during bulk electrolysis and theoretical O_2 assuming Faradaic behavior (red). Black arrow indicates the termination of electrolysis.

period due to capacitance (Figure S6), j decreases slowly to reach a stable regime at 35−40% of the initial catalytic current after one day. This deactivation occurs only in brand new electrodes, and it is probably due to the mechanical loss of poorly attached crystallites. Catalytic deactivation would be a monotonic process, and it should continue at a constant pace. However, the stable catalytic current persists in the long term, without any further sign of deterioration. Successive electrolyses in new buffer solutions reach consistent stable currents right after capacitance (Figure 4), and j follows a very slow deactivation rate of <3% per day, probably due to changes in pH. We calculated the number of redox-active sites on a modified electrode at this stage and found $\Gamma = 0.30 \pm 0.06$ nmol/cm^2, consistent with the evolution of the catalytic current. For example, we can estimate a persistent TOF = 0.7 s^{-1} under an applied potential of 1.41 V (vs NHE) taking into account final coverage, in very good agreement with the initial TOF = 0.9 s^{-1}.

The efficiency of the process is quantitative. O_2 evolution, quantified with a fluorescence probe, matches the theoretical amount calculated from Faraday's law (Figure 4b) for a $4e^-$ redox process. This confirms that no competing redox reactions are taking place, and that j is quantitative for oxygen production. Thus, a constant daily production at over 60 000 cycles can be reached by this catalyst, 5000 L of O_2 per day, per gram of CoHCF catalyst, at neutral pH and ambient conditions.

We can derive some comparisons between the activity of CoHCF and cobalt oxides,[37] arguably the best heterogeneous WOCs reported to date. A TOF = 2.6×10^{-3} s^{-1} was reported

dx.doi.org/10.1021/ja406242y | J. Am. Chem. Soc. 2013, 135, 13270−13273

for a cobalt oxide film at pH 7 and η = 410 mV. Our CoHCF catalyst exhibits already the same TOF at just η = 305 mV. Of course, this comparison is quite rough because of the very different morphology of the films. In both cases TOF is referred to bulk content, and a different surface-to-bulk ratio would significantly affect the results. Still, our data show that CoHCF is at least competitive in kinetic terms with respect to the oxide counterparts. However, the reported maximum current densities for oxides are higher. We rationalize this because of the higher surface coverage. CoO_x films reach 1 mA/cm^2 just above 410 mV, but with loadings in the μmol/cm^2 range, whereas Γ is below 0.5 nmol/cm^2 in the CoHCF films. We can estimate that 1 mA would be reached at just 400 mV overpotential with CoHCF coverages about 2.5 nmol/cm^2.

The participation of any adventitious cobalt oxide on the CoHCF-modified electrodes can be ruled out for several reasons according to experimental evidence. The films exhibit all the expected features of a Prussian blue material, including spectroscopic and crystallographic data. Cobalt oxide cannot form at the derivatization potential, since a higher potential is needed for Co oxide formation.[37] No metallic cobalt remains on the electrode after derivatization, as confirmed by cyclic and differential pulse voltammetry (Figure S1). Current intensity does not increase during water electrolysis, and this also discards the *in situ* hypothetical formation of a more active catalyst.[38] The distinct Tafel slope of CoHCF when compared with Co oxides also suggests a different catalytic mechanism. Finally, the apparently faster catalytic activity found for CoHCF indicates that major oxide contamination would be needed to match these results, and this is inconsistent with all the structural, spectroscopic, and electrochemical data.

After bulk water electrolysis, the CoHCF electrodes have lower density of crystallites, which now show rounded edges (Figure S4). EDX analysis indicates that the Fe/Co ratio remains unchanged, and no traces of phosphate appear. CoO_x films incorporate phosphate from solution during water oxidation, in a self-repairing process.[11] Therefore, the absence of a P absorbance peak is another experimental indication of no oxide participation. The X-ray powder diffraction pattern shows good crystallinity and only two small differences. The diffraction peaks are displaced to higher angles, leading to a smaller unit cell a = 9.90 ± 0.05 Å, and the reflection (220) has decreased its relative intensity (Figure 2). Both can be attributed to the oxidation of CoHCF. Co^{III} centers possess smaller radii, and their presence requires the loss of interstitial potassium cations that scatter in-phase with the reflection (220).[35] In its oxidized state, the electrodes show purple color (Figure S2), and the IR spectrum shows two bands in the cyanide stretch region (Figure S2) at 2076 and 2125 cm^{-1}, the latter assigned to the Fe^{II}−CN−Co^{III} bridge.[36] The original color is recovered by reduction at the derivatization potential, and the same catalytic performance is exhibited by the oxidized and reduced forms.

In summary, metallic hexacyanometallates represent a novel class of heterogeneous water oxidation catalysts. Cobalt hexacyanoferrate shows very promising features: it is formed from Earth-abundant metal ions in aqueous solution; it works at neutral pH and ambient conditions; it is robust in turnover conditions; and it is fast enough to compete with state-of-the-art cobalt oxides. Our data demonstrate how a CoHCF-modified electrode works for days, and probably weeks, maintaining constant rates without significant fatigue. At the same time, CoHCF offers the additional advantages of molecule-based materials, not commonly associated with metal oxides: well-defined crystal structure, low density, flexibility, easy processability, and transparency to visible light. The latter is due to the localized electronic structure of coordination polymers (insulators), and this could be of particular interest for its incorporation in light-harvesting devices. Although total current densities are low for the required technological targets, this should be easily overcome by increasing surface coverage. Higher loadings can be reached by improved processing on more compatible electrode surfaces or as amorphous films. This is currently under study.

■ ASSOCIATED CONTENT

Ⓢ Supporting Information

Experimental details including methods and spectroscopic, electrochemical, and structural characterization data. This material is available free of charge via the Internet at http://pubs.acs.org.

■ AUTHOR INFORMATION

Corresponding Author

jrgalan@iciq.es

Author Contributions

[§]S.P. and S.G.F. contributed equally to this work.

Notes

The authors declare no competing financial interest.

■ ACKNOWLEDGMENTS

We thank the EU (ERC Stg grant CHEMCOMP), the Spanish Ministerio de Economia y Competitividad (Grant CTQ2012-34088), and the ICIQ Foundation for financial support. We thank Prof. Leroy Cronin for helpful discussion.

■ REFERENCES

(1) Dau, H.; Limberg, C.; Reier, T.; Risch, M.; Roggan, S.; Strasser, P. *ChemCatChem* **2010**, *2*, 724−761.

(2) Inoue, H.; Shimada, T.; Kou, Y.; Nabetani, Y.; Masui, D.; Takagi, S.; Tachibana, H. *ChemSusChem* **2011**, *4*, 173−179.

(3) Liu, X.; Wang, f. Y. *Coord. Chem. Rev.* **2012**, *256*, 1115−1136.

(4) Hocking, R. K.; Brimblecombe, R.; Chang, L.-Y.; Singh, A.; Cheah, M. H.; Glover, C.; Casey, W. H.; Spiccia, L. *Nat. Chem.* **2011**, *3*, 461−466.

(5) Minguzzi, A.; Fan, F.-R. F.; Vertova, A.; Rondinini, S.; Bard, A. J. *Chem. Sci.* **2012**, *3*, 217−229.

(6) Sivula, K.; Le Formal, F.; Grätzel, M. *ChemSusChem* **2011**, *4*, 432−449.

(7) Suntivich, J.; May, K. J.; Gasteiger, H. A.; Goodenoigh, J. B.; Shao-Horn, Y. *Science* **2011**, *334*, 1383−1385.

(8) Maeda, K.; Ohno, T.; Domen, K. *Chem. Sci.* **2011**, *2*, 1362−1368.

(9) Smith, R. D. L.; Prévot, M. S.; Fagan, R. D.; Zhang, Z.; Sedach, P. A.; Siu, M. K. J.; Trudel, S.; Berlinguette, C. P. *Science* **2013**, *340*, 60−63.

(10) Kanan, M. W.; Surendranath, Y.; Nocera, D. G. *Chem. Soc. Rev.* **2008**, *321*, 109−114.

(11) Kanan, M. W.; Nocera, D. G. *Science* **2008**, *321*, 1072−1075.

(12) Gerken, J. B.; McAlpin, J. G.; Chen, J. Y. C.; Rigsby, M. L.; Casey, W. H.; Britt, R. D.; Stahl, S. S. *J. Am. Chem. Soc.* **2012**, *133*, 14431−14442.

(13) Pijpers, J. J. H.; Winkler, M. T.; Surendranath, Y.; Buonassisi, T.; Nocera, D. G. *Proc. Natl. Acad. Sci. U.S.A.* **2011**, *108*, 10056−10061.

(14) Steinmiller, E. M. P.; Choi, K. S. *Proc. Natl. Acad. Sci. U.S.A.* **2009**, *106*, 20633−20636.

(15) Surendranath, Y.; Reece, S. R.; Nocera, D. G. *Energy Environ. Sci.* **2011**, *4*, 499−504.

(16) Chen, J.; Selloni, A. *J. Phys. Chem. Lett.* **2012**, *3*, 2808−2814.

(17) Esswein, A. J.; McMurdo, M. J.; Ross, P. N.; Bell, A. T.; Tilley, T. D. *J. Phys. Chem. C* **2009**, *113*, 15068−15072.
(18) Yeo, B. S.; Bell, A. T. *J. Am. Chem. Soc.* **2011**, *133*, 5587−5593.
(19) Wee, T.-L.; Sherman, B. D.; Gust, D.; Moore, A. L.; Moore, T. A.; Liu, Y.; Scaiano, J. C. *J. Am. Chem. Soc.* **2011**, *133*, 16742−16745.
(20) Jiao, F.; Frei, H. *Angew. Chem., Int. Ed.* **2009**, *48*, 1841−1844.
(21) Pijpers, J. J. H.; Winkler, M. T.; Surendranath, Y.; Buonassisi, T.; Nocera, D. G. *Proc. Natl. Acad. Sci. U.S.A.* **2011**, *108*, 10056−10061.
(22) Nocera, D. G. *Acc. Chem. Res.* **2012**, *45*, 767−776.
(23) Dunbar, K. R.; Heintz, R. A. *Prog. Inorg. Chem.* **1997**, *45*, 283−391.
(24) Buser, H. J.; Schwarzenbach, D.; Petter, W.; Ludi, A. *Inorg. Chem.* **1977**, *16*, 2704−2710.
(25) Ferlay, S.; Mallah, T.; Ouahes, R.; Veillet, P.; Verdaguer, M. *Nature* **1995**, *378*, 701−703.
(26) DeLongchamp, D. M.; Hammond, P. T. *Adv. Funct. Mater.* **2004**, *14*, 224−232.
(27) Kaye, S. S.; Long, J. R. *Catal. Today* **2007**, *120*, 311−316.
(28) Ohkoshi, S.-i.; Nakagawa, K.; Tomono, K.; Imoto, K.; Tsunobuchi, Y.; Tokoro, H. *J. Am. Chem. Soc.* **2010**, *132*, 6620−6621.
(29) Wang, J. *Chem. Rev.* **2008**, *108*, 814−825.
(30) Itaya, K.; Uchida, I.; Neff, V. D. *Acc. Chem. Res.* **1986**, *19*, 162−168.
(31) Purnaghi-Azar, M. H.; Sabzi, R. *J. Solid State Electrochem.* **2002**, *6*, 553−559.
(32) Xun, Z.; Cai, C.; Xing, W.; Lu, T. *J. Electroanal. Chem.* **2003**, *545*, 19−27.
(33) Heli, H.; Eskandari, I.; Sattarahmady, N.; Moosavi-Movahedi. *Electrochim. Acta* **2012**, *77*, 294−301.
(34) de Tacconi, N. R.; Rajeshwar, K.; Lezna, R. O. *Chem. Mater.* **2003**, *15*, 3046−3062.
(35) Bleuzen, A.; Lomenech, C.; Escax, V.; Villain, F.; Varret, F.; Cartier dit Moulin, C.; Verdaguer, M. *J. Am. Chem. Soc.* **2000**, *122*, 6648−6652.
(36) Lezna, R. O.; Romagnoli, R.; de Tacconi, N. R.; Rajeshwar, K. *J. Phys. Chem. B* **2002**, *106*, 3612−3621.
(37) Surendranath, Y.; Kanan, M. W.; Nocera, D. G. *J. Am. Chem. Soc.* **2010**, *132*, 16501−16509.
(38) Stracke, J. J.; Finke, R. G. *J. Am. Chem. Soc.* **2011**, *133*, 14872−14875.